

## An $^{57}\text{Fe}$ Mössbauer Effect Study of Ankerite

E. De Grave<sup>1\*</sup> and R. Vochten<sup>2</sup>

<sup>1</sup> Laboratory of Magnetism, Gent State University, Proeftuinstraat 86, 9000 Gent, Belgium

<sup>2</sup> Laboratory for Physical and Chemical Mineralogy, University of Antwerp, Middelheimlaan 2, 2020 Antwerpen, Belgium

**Abstract.** A natural sample of ankerite has been characterized by chemical analysis, X-ray diffraction and differential thermal analysis. The composition was found to be  $(\text{Ca}_{1.11}\text{Mg}_{0.50}\text{Fe}_{0.33}\text{Mn}_{0.09})[\text{CO}_3]_{1.99}$ .  $^{57}\text{Fe}$  Mössbauer effect measurements were performed at temperatures between 4.2 and 400 K. At low temperatures ( $T < 25$  K) relaxation effects are clearly dominant. The temperature dependence of the center shift is remarkably well reproduced by a model based on the Debye approximation of the lattice vibrations. In contrast, the temperature dependence of the quadrupole splitting cannot be described by any reasonable crystal field model. It is argued that an orbit-lattice coupling might explain the observed quadrupole splittings. A spectrum recorded in an applied field of 6 T reveals a positive electric field gradient from which an orbital doublet ground state is concluded. Highly anisotropic field reductions are derived but cannot be quantitatively explained due to a lack of knowledge concerning the magnetic structure of ankerite. The line widths decrease significantly with increasing temperature which is only partly due to the decreasing Mössbauer fraction.

### Introduction

Ankerite is a mineral belonging to the dolomite group of trigonal carbonates which has the general composition  $\text{Ca}(\text{Fe}, \text{Mg})(\text{CO}_3)_2$ . Dolomites with a very low Fe content usually exhibit a distinctive X-ray reflection line at  $\approx 4.03\text{Å}$ , arising from the (100) planes, which is absent in the case of high Fe contents (Howie and Broadhurst 1958). The latter samples are termed ankerites, the former ones dolomites.

The space group of dolomite is  $R\bar{3}$  (Wasastjerna 1924). The Ca and (Mg, Fe) cations are alternately situated along any threefold axis and are octahedrally co-ordinated by oxygen. Smythe and Dunham (1947) noted that careful chemical analyses usually reveal a Ca content in excess of that required by the ideal chemical formula. It is suggested that this excess of Ca substitutes for (Fe, Mg) although the two sites involved are, due to the ordering, structurally inequivalent.

Minerals from the dolomite series have a significant mineralogical and technological importance. They are e.g.

frequently found in connection with coals (Lefelhocz et al. 1967; Williamson and Melchior 1980; Montano 1981), oil shales (Melchior et al. 1982) and petroleum source rocks (Mørup and Lindgreen 1982). Because of its specificity,  $^{57}\text{Fe}$  Mössbauer spectroscopy might be very suitable to identify the dolomite-ankerite species and to distinguish them from other iron-containing carbonates, such as siderites and iron-substituted calcites.

In the present study, the temperature dependence of the Mössbauer effect in a well-characterized natural ankerite sample (origin: Stolzenbourg, Luxembourg) is discussed. Some fundamental processes, observed at very low temperatures ( $T < 20$  K), are briefly mentioned but a detailed quantitative interpretation of these effects, being of no relevance from the mineralogical point of view, will be presented in a forthcoming paper.

### Experimental

The FeO content of the ankerite mineral was determined titrimetrically using  $\text{K}_2\text{Cr}_2\text{O}_7$  (Pratt 1894). The Ca, Mg and Mn concentrations were obtained from the atomic absorption spectra collected with a Perkin Elmer 400 spectrophotometer.  $\text{CO}_2$  was analysed according to a method described by Vogel (1962):

X-ray diffraction measurements were performed with a Phillips PW 1140 diffractometer equipped with a monochromator. The radiation used was  $\text{CuK}\alpha$ .

DTA curves were recorded with a Dupont instruments. The atmosphere was  $\text{N}_2$  and the heating rate  $10^\circ\text{C}/\text{min}$ .

$^{57}\text{Fe}$  Mössbauer spectra at temperatures between 80 and 480 K and in an applied magnetic field were obtained on a conventional time-mode spectrometer with constant acceleration drive and a triangular reference signal.  $^{57}\text{Co}$  in a Rh matrix was used as radiation source. The absorber consisted of the finely ground ankerite, mixed with very pure carbon and spread out over the support in a uniform thickness of approximately  $10\text{ mg Fe}/\text{cm}^2$  (with an estimated inaccuracy of 10%). More details about the spectrometer and its calibration may be found in a recent paper by De Grave et al. (1984).

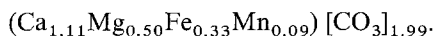
Spectra at temperatures below 80 K and down to  $\approx 11$  K were obtained on a different absorber ( $\approx 6\text{ mg Fe}/\text{cm}^2$ , mixed with sugar powder) mounted in a closed cycle cryostat. The micro-processor controlled spectrometer with interferometric calibration has been described in great detail in a previous paper (De Grave et al. 1982).

\* Research Associate with the National Fund for Scientific Research (Belgium)

The Mössbauer parameters were evaluated by a least-squares fitting of a sum of Lorentzian-shaped absorption lines to the experimental data. Mössbauer line shape calculations, aimed to explain the high field spectrum, were performed according to a method described by Varret (1976) in which anisotropic field reductions are taken into account. Due to the large computing times, iteration of the parameters was not attempted in this latter case.

## Results

*A. Characterization of the sample.* The weight percentages of FeO, CaO, MgO, MnO and CO<sub>2</sub>, obtained from chemical analysis, are 11.94, 31.07, 10.14, 3.06 and 43.79, respectively, leading to a formula:



Such a composition lies in the ankerite field as defined in the phase diagram of Cole et al. (1978). The lattice constants, calculated according to the method of Cohen (1935), were found to be  $a=b=4.8410$  (23) Å and  $c=16.162$  (23) Å, while values of 4.824 (3) and 16.132 (19) respectively are reported for the JCPDS ankerite (No.33-282). Using the program of Visser (1969), all 19 reflections observed were indexed.

The DTA curve exhibits three endothermic reactions at 760, 780 and 830° C respectively, which is characteristic for ankerite (Warne et al. 1981).

*B. <sup>57</sup>Fe Mössbauer Spectroscopy.* A typical Mössbauer spectrum for the ankerite sample is shown in Figure 1 ( $T=480$  K). The doublet is clearly asymmetric and it was found that the asymmetry changes drastically with the applied absorber preparation: for the 10 mg Fe/cm<sup>2</sup> absorber with carbon mixing, the area ratio of the low-velocity peak against the high-velocity peak is  $0.85 \pm 0.01$  at all temperatures while for the 6 mg Fe/cm<sup>2</sup> absorber with sugar mixing, no significant asymmetry was detected. This observation indicates that the effect cannot be ascribed to anisotropic Mössbauer fractions (i.e. the well-known Goldanskii-Karyagin effect), but that it rather arises from preferred orientations ("texture") of the crystallites, and therefore of the axis of the *electric field gradient* (EFG). This is corroborated by the spectral shape, shown in Figure 2, obtained when the absorber-plane makes the so-called "magic angle" (54.7°) with the incident  $\gamma$ -rays (Ericsson and Wäppling 1976).

At temperatures below  $\approx 25$  K, a different type of asymmetry appears in the Mössbauer spectra. An example of it is shown in Figure 3 and refers to  $T=12$  K. Attempts to fit such spectra with a sum of two independent Lorentzians revealed considerable deviations from the observed line shapes. Simulations based on the relaxation model of Blume (1968), however, reproduced the experimental line shapes remarkably well. A detailed analysis of the spectra in this low-temperature region and the interpretation of the relaxation processes will be presented in a forthcoming paper.

Figure 4a shows the Mössbauer spectrum at  $T=180$  K in longitudinal external magnetic field of 6T. The line shape, plotted in Figure 4b, was calculated as mentioned in the previous Section, using the hyperfine interaction data derived from the zero-field spectra and a positive sign of the EFG. The anisotropic field reductions were  $H_{IX}=H_{IY}=-0.6$  T and  $H_{IZ}=-12.5$  T. The agreement between the

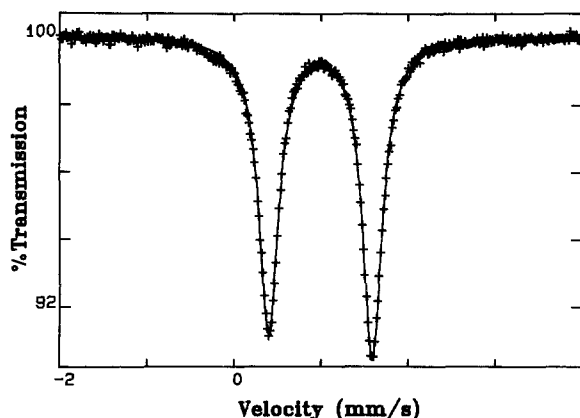
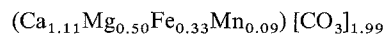


Fig. 1. Mössbauer spectrum at 480 K for ankerite



Full line represents the calculated spectrum

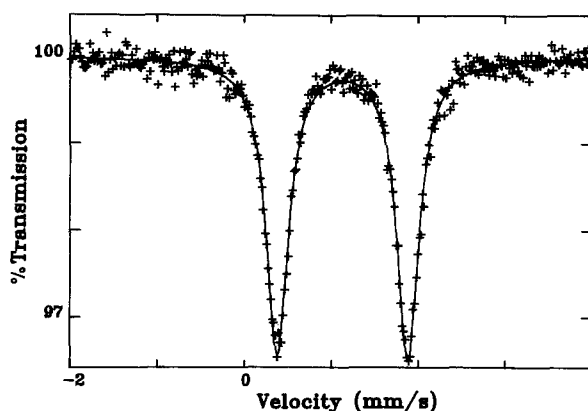


Fig. 2. Mössbauer spectrum at room temperature of the ankerite sample with the  $\gamma$ -rays making the "magic angle" with the plane of the absorber. Full line represents the calculated spectrum

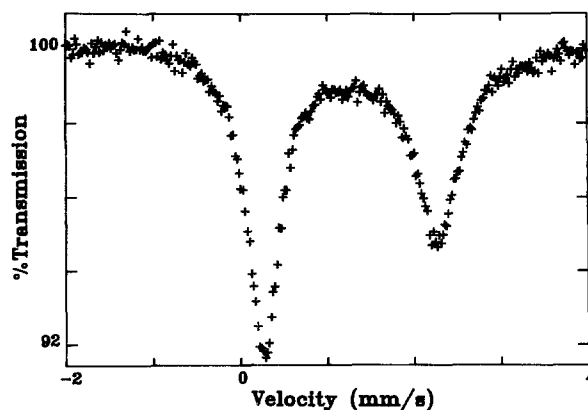


Fig. 3. Mössbauer spectrum at 12 K for ankerite

experimental and calculated intensities is, as seen from Figure 4, not complete. The major reason for the observed deviations is probably to be ascribed to the asymmetry, arising from the presence of texture effects, which is not included in the computer program.

The center shift  $\delta$  (versus metallic Fe at room temperature) and the quadrupole splitting  $\Delta E_Q$  are plotted against the temperature  $T$  in Figure 5 and Figure 6 respectively. The full lines represent the theoretical curves calculated

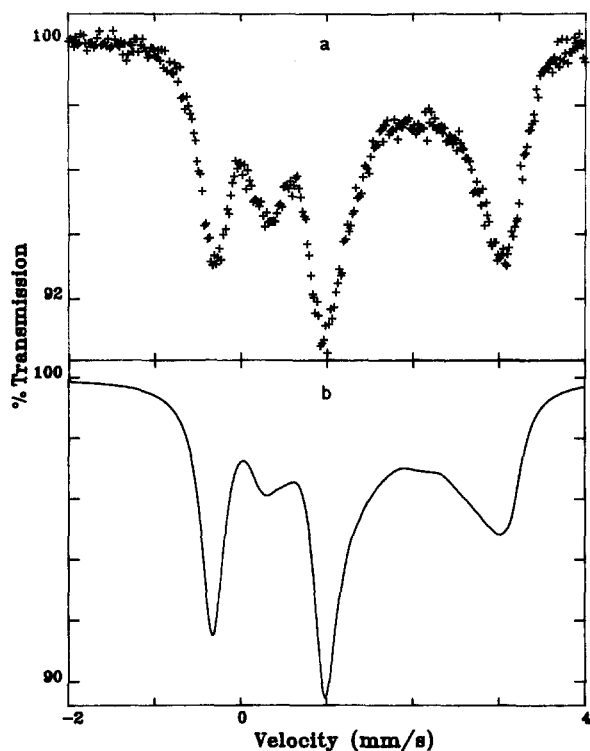


Fig. 4a, b. Ankerite Mössbauer spectrum at 180 K in an external magnetic field of 6 T. (a): experimental data. (b): simulated line shape assuming a positive EFG

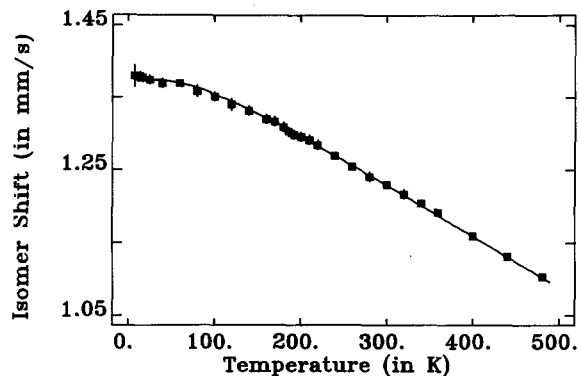


Fig. 5. Isomer shift  $\delta$  (versus metallic iron at room temperature) plotted as a function of temperature. Full line is the calculated temperature dependence on the basis of the Debye approximation for the lattice vibrations

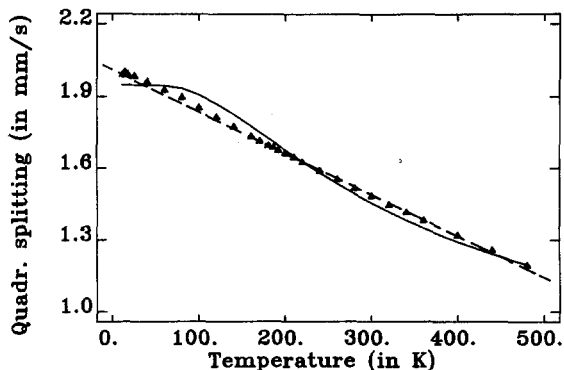


Fig. 6. Temperature dependence of the quadrupole splitting  $\Delta E_Q$  of  $\text{Fe}^{2+}$  in ankerite. Full line represents the theoretical curve calculated from the crystal field model. Broken line serves as a guide for the eye

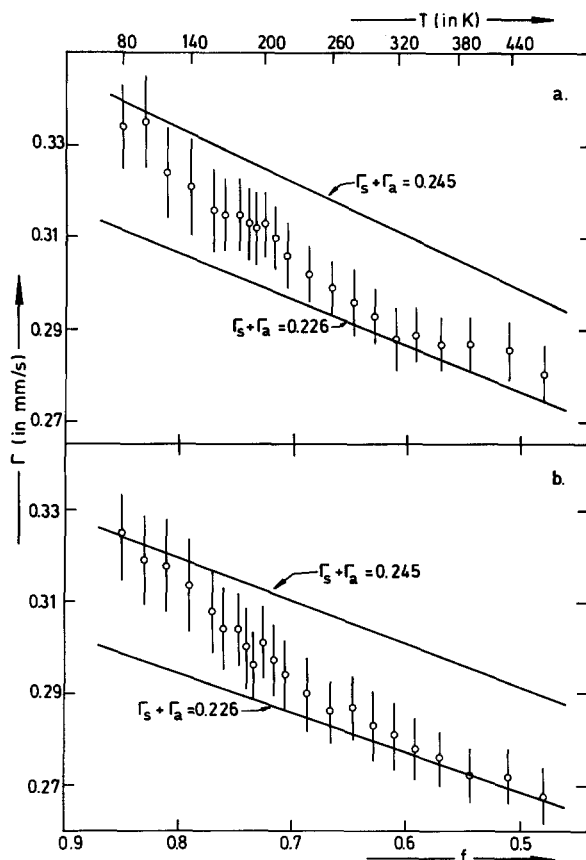


Fig. 7a, b. Line width  $\Gamma$  (FWHM) of the positive- (a) and negative- (b) velocity peak as a function of temperature  $T$  (upper scale) and Mössbauer fraction  $f$  (lower scale). Full lines represent calculated dependences for two different  $\Gamma_s + \Gamma_a$  values

from existing models and will be discussed in the next Section. Figure 7 contains the line width  $\Gamma$  of both absorption-lines for temperatures  $T > 80$  K. They are plotted as a function of the Mössbauer fraction  $f$  (cf. below).

## Interpretation and Discussion

**A. Center Shift.** The temperature dependence of the center shift  $\delta$  is due to the second-order Doppler shift  $\delta_{\text{SOD}}$  arising from the non-zero average of the quadratic velocity of the absorbing nuclei. The full curves plotted in Figure 5 represent the theoretical expression  $\delta = \delta_i - \delta_{\text{SOD}}$  fitted to the observed  $\delta$  values for 28 different temperatures. The intrinsic isomer shift  $\delta_i$  is determined by the s-electron density at the nucleus and may be regarded as a constant.  $\delta_{\text{SOD}}$  was evaluated in terms of the Debye model for the lattice vibrations (Pound and Rebka 1960) which contains the physical quantity  $\theta_D$  called the Debye temperature of the solid. Its value was fitted to be 300 K. By subtracting  $\delta_{\text{SOD}}$  from the observed  $\delta$ 's for each of the applied temperatures, the intrinsic isomer shift was found to be  $(1.456 \pm 0.005)$  mm/s at all temperatures. A physical meaning behind the obtained Debye temperature  $\theta_D$  should not be searched for at the moment but its value might become relevant as soon as similar results for other members of the dolomite-ankerite system are known.

The center shift, relative to Fe, is found to be 1.25 mm/s at 300 K and 1.36 mm/s at 80 K. These values are in excel-

lent agreement with the results for ankerite found in coals (Lefelhocz et al. 1967) and in several types of oil shales (Shiley et al. 1981; Melchior et al. 1982). The RT value further very well fits in the range 1.23–1.28 mm/s observed for different kinds of iron-containing carbonates (Musić et al. 1980; Srivastava 1983). The value of 0.85 mm/s quoted by Gallagher et al. (1981), is, in our opinion, the result of an error in converting the observed isomer shift to the metallic iron reference.

**B. Quadrupole Splitting.** From crystallographic considerations, the symmetry of the EFG may be expected to be trigonal. The positive sign then indicates that the octahedral co-ordination of the central  $\text{Fe}^{2+}$  ion is elongated along the trigonal axis (Dockum and Reiff 1979), giving rise to the orbital doublet ground state  ${}^5E_g$  with ( $t^+$ ,  $t^-$ ) wave functions. The magnitude of the quadrupole splitting, being lower than 2 mm/s, confirms this degeneracy of the electronic ground state. The  $\text{Fe}^{2+}$  electronic structure in ankerite is therefore very similar to the one in  $\text{FeCO}_3$  (Hang Nam Ok 1969) and in iron-substituted  $\text{CaCO}_3$  and  $\text{CdCO}_3$  (Price and Srivastava 1976).

The temperature dependence of the ferrous EFG is due to thermal population of the first excited electronic state (Ingalls 1964). For ankerite, this state is the orbital singlet  ${}^5A_{1g}$  which causes a negative EFG at the nucleus, whereas the ground state  ${}^5E_g$  contributes a positive one with half the magnitude of the  ${}^5A_{1g}$  value. If  $\Delta_3$  is the energy separation between the  ${}^5E_g$  and  ${}^5A_{1g}$  states, the temperature dependence of  $\Delta E_Q$  may be expressed as (Bancroft 1973):

$$\Delta E_Q(T) = \Delta E_Q^0 \alpha^2 \frac{1 - \exp(-\Delta_3/kT)}{1 - \exp(-\Delta_3/kT)} + \Delta E_Q^1 \quad (1)$$

which does not include spin-orbit coupling.  $\Delta E_Q^0$  is the quadrupole splitting due to a pure orbital singlet and equals 4.80 mm/s (Spiering et al. 1974). The factor  $\alpha^2$  arises from covalency effects and is usually between 0.6 and 0.9 (Bancroft 1973). It is believed that  $\alpha^2$  for ankerite is somewhat higher than 0.8. This estimation is based upon the comparison of the intrinsic isomer shift with the value recently obtained for  $\text{Fe}^{2+}$  in chloritoid (De Grave et al. 1984).  $\delta_1$  indeed increases with decreasing covalency (i.e. increasing  $\alpha^2$ ) and was found to be smaller in the latter mineral by about 0.08 mm/s whereas  $\alpha^2$  for two chloritoid samples was evaluated as 0.81. The higher degree of covalency in chloritoid may be explained by the shorter iron-oxygen bond length in this mineral, i.e. 2.16 Å (Hanscom 1980) as compared to 2.30 Å (Povarennykh 1972) for ankerite. The lattice term  $\Delta E_Q^1$  is, to a first approximation, constant with temperature unless a change in site symmetry should occur for which, however, there is no indication whatsoever.

Fitting (1), with  $\alpha^2$  fixed to 0.85, to the experimental data (full curve in Fig. 6) yields  $\Delta_3 = 370 \text{ cm}^{-1}$  and a lattice contribution of zero within the estimated error limits of the computation (0.05 mm/s). The agreement with the experimental data is, however, rather poor and, as indicated by the broken line in Figure 6, a linear dependence would better fit the observations.

An almost linear decrease of the  ${}^{57}\text{Fe}$  quadrupole splitting with increasing temperature has been observed before in some other iron-containing carbonates as well (Nagy et al. 1975; Srivastava 1983) and, according to these authors, could not be reproduced by any reasonable crystal

field model either. A possible explanation for this peculiar effect was put forward by Price (1978) in terms of an orbit-lattice interaction which results in a temperature dependent admixture between the  ${}^5A_{1g}$  and  ${}^5E_g$  states, causing the ferrous EFG to decrease much faster than expected from the simple crystal field model. The orbit-lattice interaction is related to the co-ordination of the ferrous ion and this could explain the significant difference in temperature dependence of the EFG observed for  $\text{FeCO}_3$  and  $\text{Fe:MgCO}_3$  on the one hand, and for  $\text{Fe:CaCO}_3$ ,  $\text{Fe:CdCO}_3$  and  $\text{Ca(Fe, Mg)(CO}_3)_2$  on the other hand. Due to the large ionic radii of Cd and Ca, the latter compounds indeed have considerably higher unit cell dimensions (Bragg 1965) and this feature might somehow enhance the vibronic coupling and, therefore, cause a more pronounced temperature dependence of the electric field gradient.

**C. Anisotropic Field Reductions.** The large difference between the field-reduction parameters  $H_{IX} = H_{IY}$  and  $H_{IZ}$  reflects the pronounced anisotropy of the magnetic properties of the material. For a paramagnetic powder in an external magnetic field,  $H_{\text{ex}}$  the effective field along the axis  $i$  ( $i = x, y, z$ ) felt by the nucleus is given by (Johnson 1967):

$$H_{\text{eff}}^i = H_{\text{ext}} (1 - r_i) \quad (2)$$

The reduction factor  $r_i$  can be very large, even several times larger than the applied field value itself (Varret 1976), and this seems to be the case for the  $z$ -component in ankerite.

At any temperature  $T$ , the reduction  $r_i$  is proportional to  $g_i H_{\text{hf}}^i(0)$  with  $g$  the spectroscopic splitting factor. As mentioned before, the electronic structure of  $\text{Fe}^{2+}$  in ankerite is possibly very similar to the one in  $\text{FeCO}_3$  for which the ground state has  $g_z \approx 10$  and  $g_x = g_y \approx 0$  (Hang Nam Ok 1969). At elevated temperatures, e.g. 180 K, the anisotropy of  $g$  will be smaller due to the thermal population of higher energy states. The anisotropy in the saturation field, however, remains and might be very considerable as well (Johnson 1967). Notwithstanding, the observed ratio  $H_{IZ}/H_{IX} \approx 20$  at 180 K seems unreasonably high but due to a lack of magnetic data for ankerite, a more quantitative interpretation is not possible at the moment.

**D. Line Widths.** As Figure 7 shows, the widths of both absorption lines decrease significantly with increasing temperature. This feature is, at least qualitatively, explained by the decreasing effective thickness  $t_A$  of the absorber, due to the decreasing Mössbauer fraction  $f$ :

$$t_A = w a_a (n_a d_a) \sigma_0 f \quad (3)$$

in which  $w$  is the relative absorption area (being 0.46 and 0.54 for the negative and positive velocity peak respectively),  $a_a$  the natural abundance of the  ${}^{57}\text{Fe}$  isotope ( $\approx 0.022$ ),  $n_a d_a$  the number of iron species per  $\text{cm}^2$  and  $\sigma_0$  the maximum resonant cross section ( $2.57 \times 10^{-18} \text{ cm}^2$ ). The Mössbauer fraction  $f$  at any temperature may be estimated from the known Debye temperature  $\theta_D$  (see e.g. Herberle 1971).

For an absorber mass of 10 mg  $\text{Fe}/\text{cm}^2$ ,  $t_A$  is always smaller than 5 so that the following formula for the observed line width  $\Gamma$  may be used (O'Connor 1963):

$$\Gamma = (\Gamma_s + \Gamma_a) (1.00 + 0.135 t_A) \quad (4)$$

with  $\Gamma_s$  the source line width and  $\Gamma_a$  the absorber line width for  $t_A \rightarrow 0$ . The straight lines in Figure 7 were calculated

according to (4) with  $(\Gamma_s + \Gamma_a)$  values of respectively 0.226 and 0.245 mm/s. The actual results are obviously not reproduced by neither one of the plotted lines. Instead, it appears as though the "zero-thickness" width  $(\Gamma_s + \Gamma_a)$  gradually decreases from 0.245 mm/s to 0.226 mm/s when the temperature is raised from 80 ( $f=0.85$ ) to 480 K ( $f=0.48$ ). It could be calculated that the effect is not an artifact due to an incorrect evaluation of the  $f$  factors. Only if those were off by about 60 percent, the observed curvature could be explained. In this case, however, unrealistic  $f$  values exceeding 1 would be obtained. Furthermore, neither the inclusion of the term in  $t_A^2$  (Frauenfelder et al. 1962), nor the polynomial of fourth degree in  $t_A$ , evaluated by Herberle (1968), can reasonably reproduce the observed temperature dependence. Therefore, it appears that, in addition to the decreasing absorber thickness, a second effect causing line narrowing at higher temperatures must be present and, according to a recent Mössbauer study on natural chloritoids (De-Grave et al. 1984), this effect might be quite general and deserves further attention.

## Conclusion

The Mössbauer effect in the present ankerite sample is in many respects very similar to the behaviour of several comparable iron-containing carbonates. Low-temperature relaxation effects, apparently well described by the Blume model, are observed. At room temperature, the isomer shift is within the range of values found for several other carbonates described in the literature. The saturation value for the quadrupole splitting is around 2 mm/s, which is very common as well. The electric field gradient is positive which is explained by a trigonal elongation of the octahedral coordination of the central  $\text{Fe}^{2+}$  ion, resulting in an orbital doublet ground state. As in many other iron carbonates, the quadrupole splitting decreases almost linearly with increasing temperature. This dependence, however, cannot be reproduced by any reasonable crystal field model and it is assumed that an orbit-lattice coupling, as suggested in the recent literature, might be responsible for the observed dependence. In that case, we must conclude that large cations such as  $\text{Ca}^{2+}$  and  $\text{Cd}^{2+}$ , enhance the coupling mechanism which in turn leads to a more pronounced decrease of the quadrupole splitting as compared to  $\text{FeCO}_3$ . The line width, finally, decreases with increasing temperature. Calculations have shown that the observed decrease can only partly be explained by the gradual decrease of the absorber thickness resulting from a decreasing Mössbauer fraction. An additional, but unknown, temperature effect must be present.

The present Mössbauer study has revealed a number of interesting and intriguing features, many of which are either only qualitatively explained or not understood at all. The most important of these features are, in our opinion, the low-temperature relaxation effects, the suggested orbit-lattice coupling and its implication on the quadrupole interaction, and the highly anisotropic field reduction. All these properties certainly deserve further experimental research efforts. In order to determine the compositional effect, the knowledge of which might help to elucidate the peculiar observations, several different ankerites and iron-substituted dolomites are now being collected and prepared for a study similar to the one reported in this paper.

*Acknowledgments.* The authors wish to thank Prof. Dr. G. Stoops (Gent State University) for his permission to use the DTA equipment present in his laboratory. EDG is very grateful to Prof. Dr. L.H. Brown (North Carolina State University) for a stay at his laboratory during which most of the low-temperature Mössbauer measurements were performed. The technical assistance of Ms. C. Van de Veire is acknowledged. Part of this work was financially supported by the Fund for Joint Fundamental Research (Belgium).

## References

- Bancroft GM (1973) Mössbauer spectroscopy. An introduction for inorganic chemists and geochemists. McGraw Hill, London, pp 110–154
- Blume M (1968) Stochastic theory of line shape: generalization of the Kubo-Anderson model. *Phys Rev* 174:351–358
- Bragg L (1965) Crystal structures of minerals, Vol 4. G Bell and Sons Ltd., London, p 127
- Cohen M (1935) Precision lattice constants from X-ray powder photographs. *Rev Sci Instrum* 6:68–74
- Cole RD, Liu J, Smith GV, Hinckley CC, Saporoschenko M (1978) Iron partitioning in oil shale of the Green River Formation, Colorado: a preliminary Mössbauer study. *Fuel* 57:514–520
- De Grave E, Bowen LH, Hedges SW (1982) Mössbauer spectroscopy with a microprocessor: a versatile software package. *Nucl Instrum Methods* 200:303–310
- De Grave E, Vanleerberghe R, Verdonck L, De Geyter G (1984) Mössbauer and infrared spectroscopic studies of Belgian chloritoids. *Phys Chem Minerals* 11:85–94
- Dockum BW, Reiff WM (1979) A high field Mössbauer study of a six coordinate iron II dithiocarbamate complex and comparison of the  $\text{Fe(II)S}_6$ ,  $\text{Fe(III)S}_6$  and  $\text{Fe(IV)S}_6$  chromophores in tris(diethyldithiocarbamate) complexation. *Chem Phys Letters* 63:32–36
- Ericsson T, Wäppling R (1976) Texture effects in  $3/2-1/2$  Mössbauer spectra. *J Phys Colloq* 37:C6-719–C6-723
- Frauenfelder H, Nagle DE, Taylor RD, Cochran DRF, Visscher WM (1962) Elliptical polarization of  $\text{Fe}^{57}$  gamma rays. *Phys Rev* 126:1065–1075
- Gallagher PK, West KW, Warne SSJ (1981) Use of the Mössbauer effect to study the thermal decomposition of siderite. *Thermochim Acta* 50:41–47
- Hang Nam OK (1969) Relaxation effects in antiferromagnetic ferrous carbonate. *Phys Rev* 185:472–476
- Hanscom R (1980) The structure of triclinic chloritoid and chloritoid polymorphism. *Am Mineral* 65:534–539
- Heberle J (1968) Linewidth of Mössbauer absorption. *Nucl Instrum Methods* 58:90–92
- Heberle J (1971) The Debye integrals, the thermal shift and the Mössbauer fraction. In: Gruverman IJ (ed) Mössbauer effect methodology, Vol 7. Plenum Press, New York London, pp 299–308
- Howie RA, Broadhurst FM (1958) X-ray data for dolomite and ankerite. *Am Mineral* 43:1210–1214
- Ingalls R (1964) Electric field gradient tensor in ferrous compounds. *Phys Rev* 133:A787–A795
- Johnson CE (1967) Hyperfine interactions in ferrous fluosilicate. *Proc Phys Soc* 92:748–757
- Lefelhocz JF, Friedel RA, Kohman TP (1967) Mössbauer spectroscopy of iron in coal. *Geochim Cosmochim Acta* 31:2261–2273
- Melchior DC, Wildeman TR, Williamson DL (1982) Mössbauer investigation of the transformations of the iron minerals in oil shale during retorting. *Fuel* 61:516–522
- Montano PA (1981) Application of Mössbauer spectroscopy to coal characterization and utilization. In: Stevens JG, Shenoy GK (eds) Mössbauer spectroscopy and its chemical applications. American Chemical Society, Washington DC, pp 135–175
- Mørup S, Lindgreen H (1982) Applications of Mössbauer spectroscopy in oil prospecting. In: Proceedings of the international

- conference on the applications of the Mössbauer effect. Indian National Science Academy, New Delhi, pp 290–292
- Musić S, Nagy-Czakó I, Vértes A, Hadžija O (1980) Mössbauer effect study of siderite and limonite ores. *Bull Soc Chim Beograd* 45:541–547
- Nagy DL, Dézsi I, Gonser U (1975) Mössbauer studies of  $\text{FeCO}_3$ . *Neues Jahrb Mineral Monatsh* 1975:101–114
- O'Connor DA (1963) The effect of line broadening of Mössbauer resonant sources and absorbers on the resonance absorption. *Nucl Instrum Methods* 21:318–322
- Pound RV, Rebka GA Jr (1960) Variation with temperature of the energy of recoil-free gamma rays from solids. *Phys Rev Letters* 4:274–277
- Povarennykh AS (1972) Crystal chemical classification of minerals, Vol 2. Plenum Press, New York London, pp 607–627
- Pratt JH (1894) On the determination of ferrous iron in silicates. *Am J Sci* 48:149–151
- Price DC (1978) Vibronic effects in Mössbauer spectra: the  $^{57}\text{Fe}$  quadrupole splitting in  $\text{FeCO}_3$ . *Aust J Phys* 31:397–420
- Price DC, Srivastava KKP (1976) Paramagnetic hyperfine structure and electronic relaxation of  $\text{Fe}^{2+}$  in  $\text{CaCO}_3$  and  $\text{CdCO}_3$ . *J Phys Colloq* 37:C6-123–C6-127
- Shiley RH, Cluff RM, Dickerson DR, Hinckley CC, Smith GV, Twardowska H, Saporoschenko M (1981) Correlation of natural gas content to iron species in the New Albany shale group. *Fuel* 60:732–738
- Smythe JA, Dunham KC (1947) Ankerites and chalybites from the northern Pennine orefield and the northeast coalfield. *Min Mag* 28:53–74
- Spiering H, Zimmerman R, Ritter G (1974) Investigation of hyperfine interaction and structure in  $\text{FeSiF}_6 \cdot 6\text{H}_2\text{O}$  by Mössbauer measurements. *Phys Status Solidi (b)* 62:123–133
- Srivastava KKP (1983) Mössbauer quadrupole splitting of  $\text{Fe}^{2+}$  in carbonates. *J Phys C: Solid State Phys* 16:L1137–L1139
- Visser JW (1969) Fully automatic program for finding the unit cell from powder data. *Appl Crystallogr* 2:89–95
- Vogel AI (1962) Textbook of quantitative inorganic analysis. Longmans, Green and Co. Ltd. London, pp 584–586
- Varret F (1976) Mössbauer spectra of paramagnetic powders under applied field:  $\text{Fe}^{3+}$  in fluosilicates. *J Phys Chem Solids* 37:265–271
- Warne SSI, Morgan DJ, Milodowski AE (1981) Thermal analysis studies of the dolomite, ferroan dolomite, ankerite series. Part 1. Iron content recognition and determination by variable atmosphere DTA. *Thermochim Acta* 50:105–111
- Wasastjerna JA (1924) The crystal structure of dolomite. *Soc Scient Fennica Comm Phys – Math II*, No 14
- Williamson DL, Melchior DC (1980) Changes in iron minerals during oil-shale retorting. In Gary JH (ed) Proceedings of the 13th oil shale symposium. Colorado School of Mines Press, Golden, Colorado, pp 337–350

Received December 12, 1984